Theoretical and Applied Climatology (2020) 141:935–946
https://doi.org/10.1007/s00704-020-03253-w

ORIGINAL PAPER

Thermal sharpening of MODIS land surface temperature using statistical downscaling technique in urban areas

Ruchi Bala[1] · Rajendra Prasad[1] · Vijay Pratap Yadav[1]

Received: 20 December 2019 / Accepted: 29 April 2020 / Published online: 18 May 2020

Abstract

The limitation of thermal satellite images at finer spatial resolution (FR) led to increased demand for developing various downscaling techniques for the generation of FR image of land surface temperature (LST) to enhance the information content. Thus, the major concern of the analysis is the thermal sharpening of MODIS-LST in various urban regions by establishing the correlation of LST with various spectral indices (SI). Various regression techniques using combination of SI were applied for the thermal sharpening of LST from MODIS data over four different Indian cities with different climate zones i.e. Bikaner, Vadodara, Hyderabad and Varanasi. The LST image from MODIS sensors at spatial resolution of 930 m was disaggregated to 100 m and accuracy was determined by comparing with the LST image of Landsat-8-TIRS at 100 m. The best combination of indices found to include both vegetation and built-up/soil indices for thermal sharpening of MODIS-LST. Further, the variation of the best combination for different cities indicates its dependence on the present land cover. The correlation coefficients (R) between the downscaled MODIS-LST image and the reference-Landsat image were found to be 0.84, 0.76, 0.83 and 0.92, whereas the RMSE values were found to be 1.27, 1.02, 0.73 and 0.62 for Bikaner, Vadodara, Hyderabad and Varanasi, respectively. The RMSE values were found remarkably below the standard deviation of each reference LST image. Therefore, the downscaling approach adopted in this study showed high potential for accurate LST mapping at FR in various urban areas.

1 Introduction

Thermal remote sensing has gained popularity for its importance in numerous applications like environmental monitoring (Liu et al. 2016; Voogt and Oke 2003; Weng 2009), forest-fire detection (Justice et al. 2002), climate change (Zhou et al. 2019; Rajasekar and Weng 2009; Rasul et al. 2017) and also for soil moisture estimation and agricultural applications (Wang and Qu 2009; Kauffman et al. 2007; Zhang et al. 2015; Nuruzzaman 2015). Various satellites containing thermal sensors, like Moderate Resolution Imaging Spectroradiometer (MODIS), Advanced Very High Resolution Radiometer (AVHRR), Landsat Thematic Mapper/Enhanced Thematic Mapper (TM/ETM+) and Landsat-8 Thermal Infrared Remote Sensing (TIRS) and Advanced Spaceborne Thermal Emission and Reflection Radiometer (ASTER), have been used for determining land surface temperature (LST) at different spatial resolution (SR) and temporal resolution (Yao et al. 2017, 2018; Julien and Sobrino 2009). Urbanization has led to the change in land cover and also increase in anthropogenic heat discharge at large scale which has significant impact on urban temperatures. The heterogeneity of land cover in urban areas has increased demand for the LST at fine spatial resolution (FR) from satellite data. The lack of satellite thermal images at FR triggered the evolution of various downscaling techniques for increase in spatial details from the original coarse-spatial resolution (CR) LST image (Zhan et al. 2013; Atkinson 2013).

The land cover indices derived from visible, near infrared (NIR) and shortwave infrared (SWIR) bands are available at FR from different optical satellite images. Hence, different disaggregation methods like Distrad model (Essa et al. 2012; Eswar et al. 2016; Kustas et al. 2003), Tsharp (Agam et al. 2007a) and PBIM algorithm (Stathopoulou and Cartalis 2009) were developed for thermal sharpening of LST using the relationship of LST with various indices. The Distrad model was developed from the relation of LST with normalized difference vegetation index (NDVI) (Kustas et al. 2003). This method was used by various researchers for thermal

✉ Rajendra Prasad
rprasad.app@itbhu.ac.in

[1] Department of Physics, Indian Institute of Technology (BHU), Varanasi, India

sharpening of LST determined from the satellite data over the vegetated or natural land covers based on relation of the LST with indices like NDVI, enhanced vegetation index (EVI) and fractional vegetation cover (FVC), and the results depict that this method worked with acceptable accuracy (Agam et al. 2007a, b; Jeganathan et al. 2011). Due to higher heterogeneity in land cover of urban areas, the LST-NDVI relation may not explain all the variations of LST in urban regions (Bonafoni 2016; Zhang et al. 2009).

Stathopoulou and Cartalis (2009) tried to downscale coarser AVHRR-LST to the SR of Landsat-TM data using PBIM method to study the surface urban heat island (SUHI) effect. Error in SUHI was decreased from 2.4 °C to 0.94 °C when determined from the downscaled MODIS-LST image in comparison with the original AVHRR-LST data. Essa et al. (2012) used the relation of LST with percent impervious surface area (%ISA) and various indices for assessment of performance of the Distrad method over urban areas using Landsat-ETM+ data. %ISA showed reasonable result when compared with other indices. Mukherjee et al. (2014) evaluated the performance of five different regression methods i.e. Distrad, Tsharp, Tsharp with local variant, least median square regression downscaling (LMSR) and pace regression for the downscaling of Landsat and MODIS-LST images using LST-NDVI over a heterogeneous region of India. The model was found suitable for the agricultural or vegetated landscapes but have limitations for sandy open areas or water bodies. Eswar et al. (2016) compared the performance of five different indices i.e. NDVI, FVC, soil-adjusted vegetation index (SAVI), modified soil-adjusted vegetation index (MSAVI) and normalized difference water index (NDWI) for downscaling LST using Distrad method. The MODIS-LST at 960 m was disaggregated to 120 m and then compared with the LST from Landsat-7 images for different sites in India. NDVI/FVC showed better result for wet areas and NDWI showed better result for dry areas. Mukherjee et al. (2017) used the LST-NDVI relation by LMSR to downscale MODIS-LST image to the SR of 250 m to study the urban heat island (UHI) effect which enhances the usage of MODIS-LST for continuous monitoring of UHI effect. Yang et al. (2017) downscaled the aggregated Landsat-8-TIRS image (360 m) to the SR of 90 m using the relation of LST with multiple scale factors in mixed land covers. The downscaled MODIS-LST image was compared with the actual Landsat-LST and satisfactory result was obtained with low RMSE (1.13 K) and high coefficient of determination (R^2) of 0.87. The spatial variability increased in the downscaled MODIS-LST image from the actual MODIS-LST image which makes it suitable for study of the UHI effect. Bonafoni (2016) used various regressive techniques from multiple indices for downscaling of the upscaled Landsat-LST and the MODIS-LST to the SR of 480, 240 and 120 m during the summer season in the urban part of Milan, Italy, and root mean square error (RMSE) was found higher for MODIS image than downscaled MODIS-LST image obtained from Landsat data.

Various previous studies have been performed on thermal sharpening from satellite images using different indices in agricultural region where LST-NDVI relation was found beneficial. The negative linear relation of LST with NDVI in agricultural areas makes it suitable for thermal sharpening in agricultural areas. However, NDVI cannot explain all variations in LST in an urban area because of the non-linear relation of LST with NDVI due to greater heterogeneity in urban areas. The relation of LST with different indices depends on the kind of land cover present in an area (Bala et al. 2018). The relation of LST with one spectral index (SI) can address the contribution of one type of land cover but may not be useful for other land cover types. Thus, the combination of different SI may be beneficial for including the contribution from different types of land covers on LST in an urban area. In the present analysis, different regression based on multiple indices has been compared for thermal sharpening of coarser MODIS-LST to FR of Landsat-8-TIRS LST data in different cities of India i.e. Bikaner, Vadodara, Hyderabad and Varanasi. The natural land cover within or outside the city also influences the relation of LST with the indices. Previous studies have also discussed different thermal sharpening methods in the heterogeneous urban land cover. Essa et al. (2012) studied that %ISA performs better for downscaling in urban areas with very high vegetation cover. Bonafoni (2016) downscaled MODIS-LST using different regressive methods and the combination of SI, i.e. $a + b \times \mathrm{NDVI}^2 + c \times \mathrm{NDBI}$, performed best for MODIS disaggregation of LST. These studies performed well in regions with vegetated rural surroundings but may not be applicable in urban cities with different natural surroundings. The four urban regions selected had different types of surrounding land covers. Hence, the present work focused on determining downscaling method that can be applicable for heterogeneous urban cities located at different climatic zones.

2 Study area and data

2.1 Study area

The study areas comprise cities from four different parts of India, i.e. Bikaner, Vadodara, Hyderabad and Varanasi shown in Fig. 1. Bikaner lies at the northwest part of India in the middle of the Thar Desert with centre coordinates 28.01° N and 73.31° E. Hyderabad lies at the southeast part of India with centre coordinates 17.37° N and 78.48° E. The city lies on small hills of grey and pink granite and also consists of numerous lakes. Vadodara lies in the west India with semi-arid region having centre coordinates 22.30° N and 73.19° E. Varanasi lies in the north part of India at the bank of river Ganges with centre coordinates 25.28° N and 82.96° E.

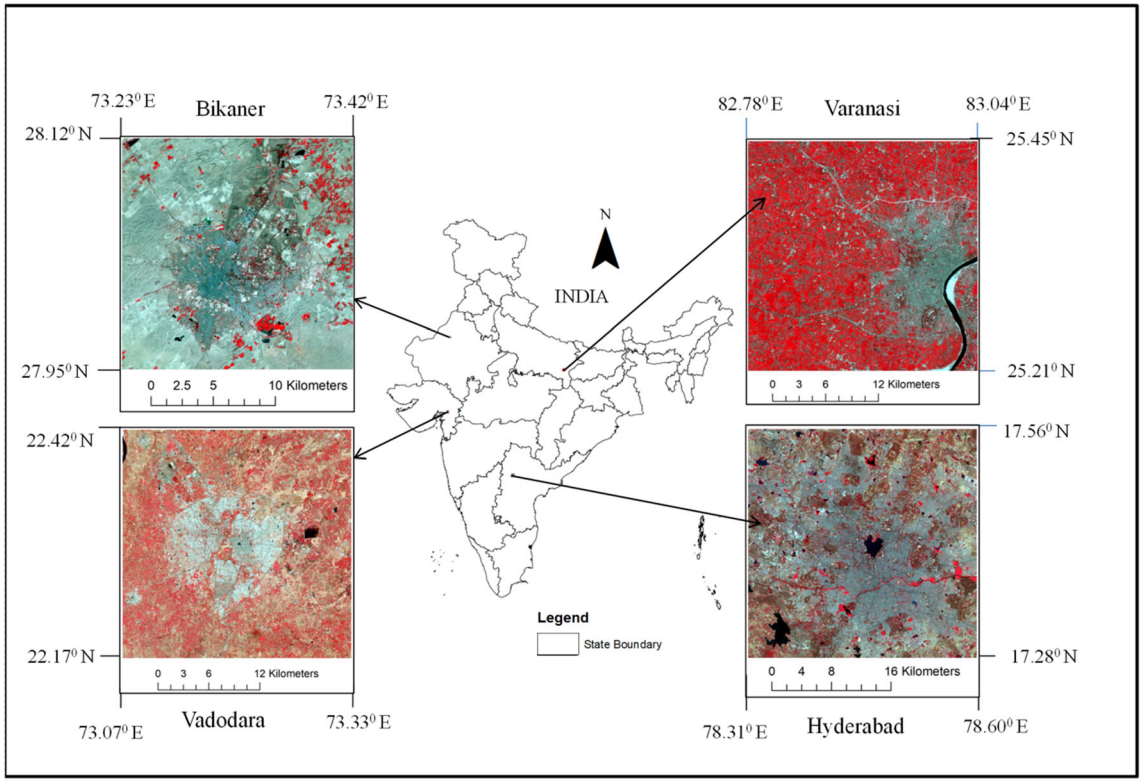

Fig. 1 Location map of the study areas. The false colour composite images obtained from Landsat 8 OLI data are shown for Bikaner, Vadodara, Hyderabad and Varanasi

Different cities are located at different climatic zones in India, i.e. subtropical arid, tropical semi-arid, tropical wet and dry and humid subtropical for Bikaner, Vadodara, Hyderabad and Varanasi respectively and consist of different neighbouring natural land covers.

The four cities were selected based on their surrounding natural land covers. The major land cover surrounding the Bikaner City is the sand/bare soil, whereas Varanasi City is surrounded mostly by vegetated land cover. The Vadodara City is surrounded by sparse vegetated or bare land and the Hyderabad City consists of various hills. The different land covers show significant variation towards LST. Thus, the present study aims at determining the downscaling methods that can be applicable in urban areas with widely different natural surroundings.

2.2 Data used and image pre-processing

MODIS-Terra-satellite LST (MOD11A1) and surface-reflectance products (MOD09A1) were downloaded from the USGS Land Processes Distributed Active Archive Center (LPDAAC) website i.e. https://lpdaac.usgs.gov/ for the locations of the study. MOD09A1 product provides 8-day composite surface reflectance from visible and infrared (IR) bands at SR of 465 m which was resampled using cubic-convolution resampling method to 500 m. MOD11A1 product provides daily per-pixel LST data at 930 m SR which was further resampled to 1000 m. The rescaling factor used to obtain MODIS-LST was 0.02. All the MODIS images were re-projected and resampled using the MODIS Reprojection Tool (MRT).

Landsat-Level-1 data products and Landsat-Higher-Level data products (Collection-1-Higher-Level) were acquired from the US Geological Survey website, i.e. https://earthexplorer.usgs.gov/ for the year 2017 during the day time of the winter season for the four study areas with the same dates as that of MODIS data. The Collection-1-Higher-Level Landsat data products were used to acquire the surface reflectance from visible and IR bands, and thermal band data was acquired from Landsat-Level-1 data products. Landsat-Level-1 data are geometric, radiometric and terrain corrected. Landsat-Collection-1-Higher-Level data are also atmospheric corrected. Landsat-8 images have SR of 30 m for bands 1 to 7 (visible, NIR and SWIR) and 100 m for thermal bands. All the images were acquired with cloud cover less than 1%. Details about the satellite data acquired are shown in Table 1.

3 Methodology

Various methods were involved in the thermal sharpening of CR MODIS-LST (930 m) to that of FR of Landsat-8-TIRS

Table 1 Details about the satellite data acquired for the study

Cities	Landsat 8 OLI dat		MODIS data (MOD11A1)		Projection UTM WGS84
	Date	Path/ row	Date	Tiles	
Hyderabad	19/02/2017	144/48	20/02/2017	h25v07	Zone - 44
Bikaner	22/02/2017	149/41	21/02/2017	h24v06	Zone - 43
Vadodara	03/03/2017	148/45	02/03/2017	h24v06	Zone - 43
Varanasi	21/02/2017	142/42	22/02/2017	h25v06	Zone - 44

data (100 m). The land cover indices from MODIS indices were computed at 500 m SR. The indices computed from Landsat-8-OLI data at 30 m SR was resampled to 100 m after aggregating to 120 m for inter-calibration process. The MODIS-LST was downscaled using the statistical downscaling technique and compared with the reference-Landsat-LST.

3.1 Calculation of indices

Nine different SI were obtained from different combinations of visible, NIR and SWIR bands of satellite data shown in Table 2. Here, ρ_n depicts the reflectance of the *n*th band of MODIS or Landsat data respectively.

3.2 LST retrieval from Landsat

Various steps are involved in the estimation of LST from Landsat data. Top of atmosphere radiance (TOA) (L_λ) was determined from the digital number (DN) using Eq. (1).

$$L_\lambda = M_L \times (\mathrm{DN}) \quad + A_L \tag{1}$$

where M_L and A_L are the multiplicative and additive rescaling factor of thermal bands which are obtained from the metadata file. The TOA radiance is a mixed signal which contains the sum of different fractions of energy emitted from both the land and atmosphere. Hence, the TOA radiance must be atmospheric corrected for the thermal band. The three major atmospheric parameters, i.e. downwelling radiances (L_d), upwelling radiance (L_μ) and the transmission (τ), were determined from an atmospheric correction tool developed by Barsi et al. (2005) for Landsat 4–5, 7 and 8 satellite data which are available at http://atmcorr.gsfc.nasa.gov/. The emissivity values were computed from NDVI as suggested by Van de Griend and Owe (1993) shown in the Table 3. Surface-leaving radiance (L_T) was estimated from TOA radiance using the above atmospheric and surface parameters shown in Eq. (2).

$$L_T = \frac{(L_\lambda) - L_\mu - \tau \times (1-\varepsilon) \times L_d}{\tau \times \varepsilon} \tag{2}$$

The L_T was further converted into LST from Planck's law as given in Eq. (3).

Table 2 Equations used for calculation of the SI

Selected indices (SI)	Landsat 8 OLI	MODIS
NDVI	$\frac{\rho_5-\rho_4}{\rho_5+\rho_4}$	$\frac{\rho_2-\rho_1}{\rho_2+\rho_1}$
SAVI	$1.5\,\frac{\rho_5-\rho_4}{\rho_5+\rho_4+0.5}$	$1.5\,\frac{\rho_2-\rho_1}{\rho_2+\rho_1+0.5}$
MSAVI	$0.5\left[(2\rho_5+1)-\sqrt{(2\rho_5+1)^2-8(\rho_5-\rho_4)}\right]$	$0.5\left[(2\rho_2+1)-\sqrt{(2\rho_2+1)^2-8(\rho_2-\rho_1)}\right]$
EVI	$2.5\,\frac{\rho_5-\rho_4}{\rho_5+6\rho_4-7.5\rho_2+1}$	$2.5\,\frac{\rho_2-\rho_1}{\rho_2+6\rho_1-7.5\rho_3+1}$
NDBI	$\frac{\rho_6-\rho_5}{\rho_6+\rho_5}$	$\frac{\rho_6-\rho_2}{\rho_6+\rho_2}$
UI	$\frac{\rho_7-\rho_5}{\rho_7+\rho_5}$	$\frac{\rho_7-\rho_2}{\rho_7+\rho_2}$
NDWI	$\frac{\rho_3-\rho_5}{\rho_3+\rho_5}$	$\frac{\rho_4-\rho_2}{\rho_4+\rho_2}$
NDSI	$\frac{\rho_7-\rho_3}{\rho_7+\rho_3}$	$\frac{\rho_7-\rho_4}{\rho_7+\rho_4}$
BI	$\frac{(\rho_6+\rho_4)-(\rho_5+\rho_2)}{(\rho_6+\rho_4)+(\rho_5+\rho_2)}$	$\frac{(\rho_6+\rho_1)-(\rho_2+\rho_3)}{(\rho_6+\rho_1)+(\rho_2+\rho_3)}$

Table 3 Estimation of land surface emissivity from NDVI values

NDVI	Land surface emissivity
NDVI < − 0.185	0.995
− 0.185 < NDVI < 0.157	0.970
0.157 < NDVI < 0.727	1.0094 + 0.047 × ln (NDVI)
NDVI > 0.727	0.990

$$T_s = \frac{K_2}{\ln\left(1 + \frac{K_1}{(L_T)}\right)} \quad (3)$$

where K_1 and K_2 are thermal constants which were obtained from metadata file.

3.3 Inter-calibration of sensors

The disaggregation process requires data from two different sensors. Here, MODIS-Landsat inter-sensor calibration is required to convert the Landsat SI into its MODIS equivalent. The linear relation was developed between indices obtained from both the sensors at CR and this relation was used to determine MODIS equivalent indices at FR (Steven et al. 2003).

3.4 Statistical downscaling technique

An empirical regression based method using the correlation of LST with suitable SI was adopted for the present analysis to downscale MODIS-LST (1 km) to the SR of Landsat-8-LST (100 m). The relation of LST with each index SI (i) was studied using the ordinary least square regression function at CR from satellite image (Bonafoni 2016).

$$\mathrm{LST_{CR}} = a_0 + a_1 \times \mathrm{SI_{CR}}(1) + a_2 \times \mathrm{SI_{CR}}(2) + \ldots\ldots + a_n \times \mathrm{SI_{CR}}(n) \quad (4)$$

$$\Delta\mathrm{LST_{CR}} = \mathrm{LST_{REF}} - \mathrm{LST_{CR}} \quad (5)$$

Here, $\mathrm{SI_{CR}}$ represents the spectral index and $\mathrm{LST_{CR}}$ represents LST at CR estimated from the satellite data. LST at FR ($\mathrm{LST_{FR}}$) could be estimated by replacing the $\mathrm{SI_{CR}}$ (i) with the corresponding SI at FR $\mathrm{SI_{FR}}$ (i). However, the effects of sharp discontinuities in the image could be neglected due to the consideration of mainly average conditions in the least square regression. This spatial variation can be considered by addition of residual of LST ($\Delta\mathrm{LST_{CR}}$) in the FR LST image. $\Delta\mathrm{LST_{CR}}$ is the difference of the calculated LST ($\mathrm{LST_{REF}}$) and $\mathrm{LST_{CR}}$ at CR shown in Eq. (5). $\mathrm{LST_{REF}}$ is the reference LST calculated from the selected indices and the corresponding coefficients derived from Eq. (4). Further, the FR LST image is obtained by applying the regression model obtained from CR LST and SI images to the FR intercaliberated SI ($\mathrm{SI_{FR}}$) shown in the Eq. (6). The residual error is added to improve the estimation accuracy.

$$\mathrm{LST_{FR}} = a_0 + a_1 \times \mathrm{SI_{FR}}(1) + a_2 \times \mathrm{SI_{FR}}(2) + \ldots. + a_n \times \mathrm{SI_{FR}}(n) + \mathrm{LST_{CR}} \quad (6)$$

The relation of LST with one SI may be useful for one type of land cover but not for other land cover types. The urban area has greater heterogeneity due to the presence of different land cover types. Thus, the linear relation of LST with a single SI may not show good behaviour in heterogeneous urban areas. The multiple linear regression uses combination of different SI which can include the contribution from different types of land covers on LST in an urban area. Thus, multiple linear regression was considered between LST and powers of SI (i) to improve the correlation.

4 Results

4.1 Downscaling of MODIS-LST using various SI employed singly

MODIS-LST was downscaled to the SR of Landsat-LST data using the disaggregation approach with nine different SI employed singly in the first and second order regression for Bikaner, Vadodara, Hyderabad and Varanasi, respectively. In order to analyze the performance of each SI, the downscaled MODIS-LST image was compared with reference-Landsat-LST image to determine RMSE for each SI for different location in study. The second order regression showed better performance than the first order. Thus, the RMSE obtained from downscaling of MODIS-LST using the second order regression is shown in Fig. 2 for comparing the potential of different indices. The variation in the behaviour of SI used in the present analysis was observed for different cities. Thus, LST relation with SI depends on the kind of land cover present.

The original MODIS-LST was compared with that of Landsat-LST at the same time and RMSE values were obtained to be 1.82, 1.22, 1.43 and 1.26 for Bikaner, Vadodara, Hyderabad and Varanasi, respectively. The RMSE values obtained from the downscaled MODIS-LST for each SI was compared with that obtained from original MODIS-LST. It was observed that the SI except SAVI, MSAVI and NDWI used in the study showed improvement in downscaling in Bikaner. All SI evaluated in this study showed improved result in Hyderabad and Vadodara, whereas all SI except NDSI showed improvement in Varanasi in downscaling of the MODIS-LST. However, lower RMSE values for NDBI, UI

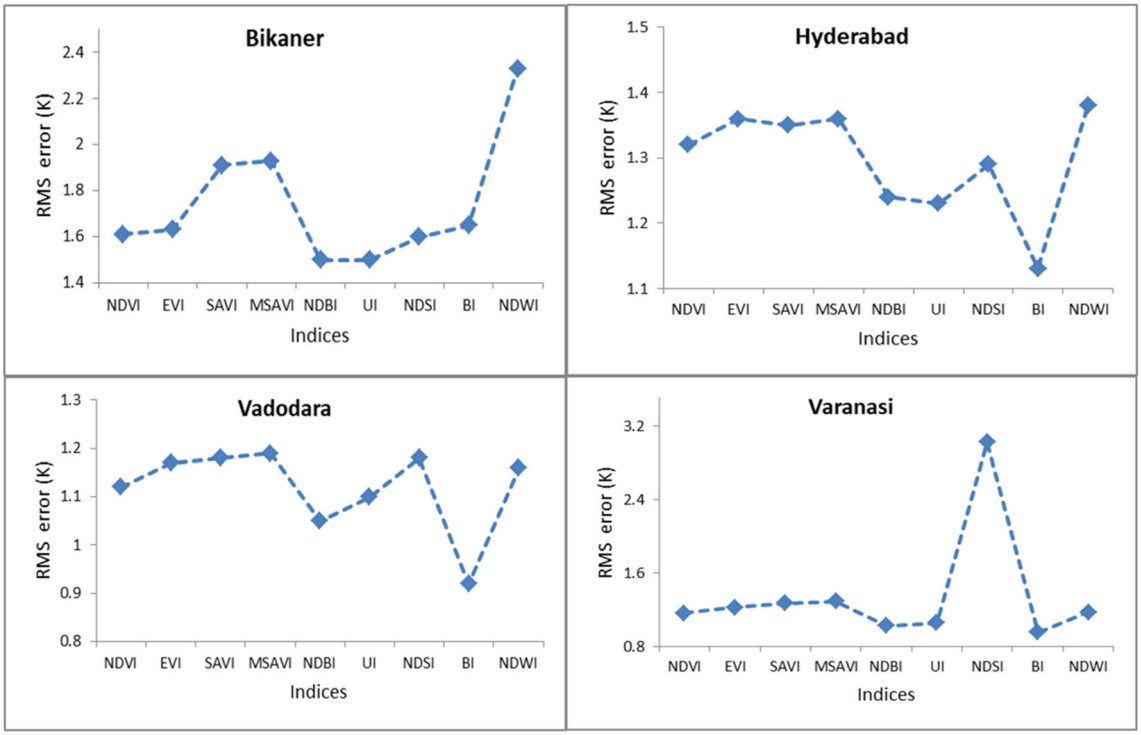

Fig. 2 RMSE of LST obtained from downscaled MODIS-LST and reference-Landsat-LST for Bikaner, Vadodara, Hyderabad and Varanasi. The downscaled image was determined from the SI used singly in the second order polynomial regression

and BI reveal good downscaling results in all the four study areas (Bonafoni et al. 2016; Bala et al. 2019).

4.2 Land cover classification and LST maps

Figure 3 represents the land cover classification map obtained using maximum likelihood classification technique with the accuracy between 82 and 89% in the four cities. Figure 4 depicts the reference-Landsat-LST map of the four study areas. The Thar Desert surrounding the urban part of Bikaner indicates higher LST than the urban part of city resulting in the formation of urban heat sink (UHS). In Hyderabad, lower LST areas within the city depict water bodies, whereas urban areas and bare regions show higher LST.

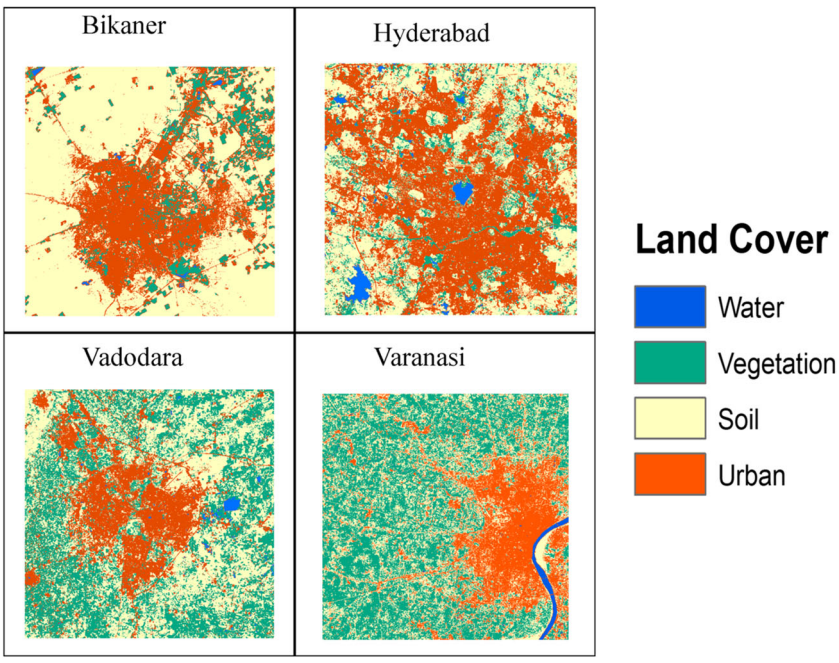

Fig. 3 Classified map of Bikaner, Vadodara, Hyderabad and Varanasi

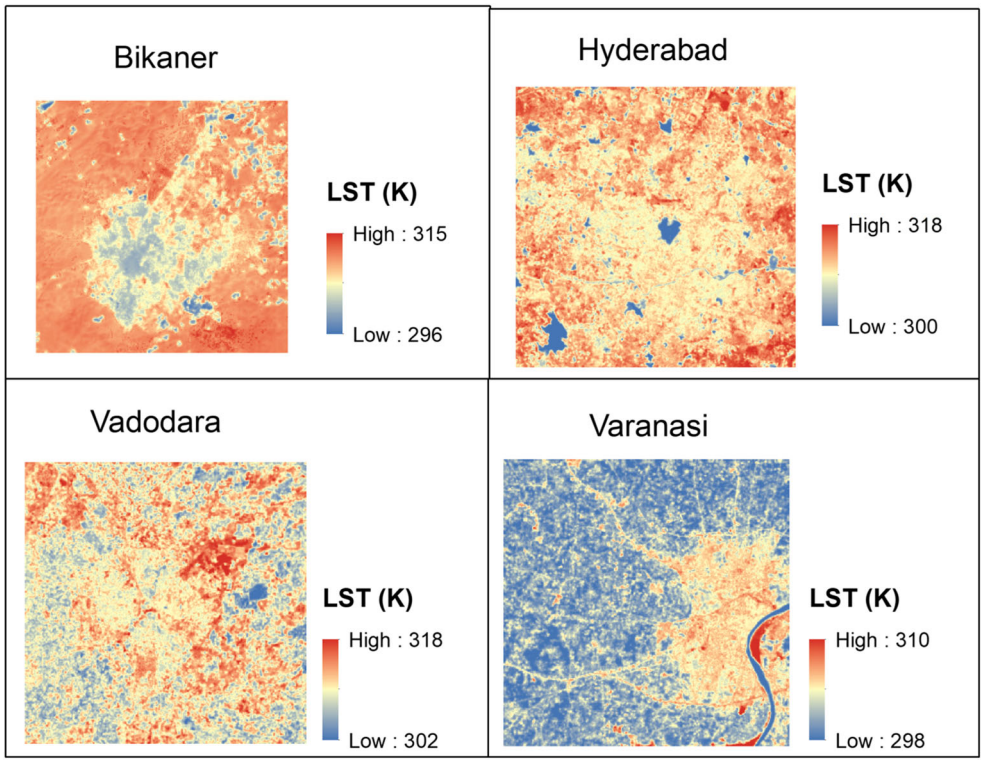

Fig. 4 Landsat-LST map of Bikaner, Vadodara, Hyderabad and Varanasi

The pixels having lowest LST in Vadodara were due to water body, whereas highest LST pixels were due to bare land. The agricultural land around the city consists of sparse vegetation which shows slightly lower LST than the urban land cover. The presence of water body and densely vegetated agricultural land surrounding the cities shows lower LST than the urban areas resulting in UHI effect.

4.3 Disaggregation of MODIS-LST using statistical downscaling technique

The different combinations of SI with different power combinations were considered in Eq. (4) and the best of downscaling results are reported in Tables 4 and 5 for the four study areas. The best regression models were obtained by determining the RMSE values shown in Fig. 2 for different combination of indices. The combination of SI as $a + b \times \mathrm{NDVI}^2 + c \times \mathrm{BI}$ was found best among the regression models for downscaling of the MODIS-LST in Hyderabad and Bikaner. Further, the combination $a + b \times \mathrm{NDVI}^2 + c \times \mathrm{NDSI}$ showed best downscaling result in Vadodara and the combination $a + b \times \mathrm{NDVI}^2 + c \times \mathrm{NDBI} + d \times \mathrm{EVI}^2$ showed best regression model for downscaling MODIS-LST in Varanasi. The regression models that exhibit improved results for downscaling of MODIS-LST were observed to vary for different cities. It

Table 4 RMSE and the correlation coefficient (R) obtained from the downscaled MODIS-LST and the reference-Landsat-LST for Bikaner and Hyderabad cities. The combinations of spectral indices with best results were reported

Bikaner			Hyderabad		
Regression	RMSE (K)	R	Regression	RMSE (K)	R
$a + b \times \mathrm{NDVI} + c \times \mathrm{NDBI}$	1.30	0.82	$a + b \times \mathrm{NDVI} + c \times \mathrm{NDVI}^2 + d \times \mathrm{NDSI}$	1.04	0.77
$a + b \times \mathrm{NDVI}^2 + c \times \mathrm{BI}$	1.27	0.84	$a + b \times \mathrm{NDVI}^2 + c \times \mathrm{BI}$	1.02	0.76
$a + b \times \mathrm{NDVI} + c \times \mathrm{NDSI}$	1.28	0.84	$a + b \times \mathrm{NDVI} + c \times \mathrm{NDSI}$	1.03	0.73
$a + b \times \mathrm{NDVI} + c \times \mathrm{NDBI} + d \times \mathrm{NDSI}$	1.28	0.83	$a + b \times \mathrm{NDVI}^2 + c \times \mathrm{BI} + d \times \mathrm{NDSI}$	1.03	0.75
$a + b \times \mathrm{NDVI}^2 + c \times \mathrm{BI} + d \times \mathrm{NDSI}$	1.27	0.82	$a + b \times \mathrm{NDVI} + c \times \mathrm{BI}$	1.03	0.76
$a + b \times \mathrm{NDVI} + c \times \mathrm{BI} + d \times \mathrm{NDSI}$	1.32	0.84	$a + b \times \mathrm{NDSI} + c \times \mathrm{NDBI}$	1.05	0.73

Table 5 RMSE and the correlation coefficient (R) obtained from the downscaled MODIS-LST and the reference-Landsat-LST for Vadodara and Varanasi cities. The combinations of spectral indices with best results were reported

Vadodara			Varanasi		
Regression	RMSE	R	Regression	RMSE	R
$a + b \times \text{NDVI}^2 + c \times \text{NDBI}$	0.74	0.82	$a + b \times \text{NDVI} + c \times \text{NDVI}^2 + d \times \text{NDBI}$	0.65	0.91
$a + b \times \text{NDVI}^2 + c \times \text{NDSI}$	0.73	0.83	$a + b \times \text{NDVI} + c \times \text{NDSI}$	0.62	0.91
$a + b \times \text{NDVI} + c \times \text{NDVI}^2 + d \times \text{NDBI}$	0.76	0.83	$a + b \times \text{EVI} + c \times \text{NDVI}^2 + d \times \text{NDBI}$	0.67	0.91
$a + b \times \text{NDVI} + c \times \text{NDBI} + d \times \text{NDSI}$	0.73	0.82	$a + b \times \text{NDVI}^2 + c \times \text{NDBI} + d \times \text{EVI}^2$	0.62	0.92
$a + b \times \text{NDVI} + c \times \text{NDBI} + d \times \text{UI}$	0.76	0.83	$a + b \times \text{NDVI}^2 + c \times \text{NDBI}$	0.67	0.91
$a + b \times \text{SAVI}^2 + \text{UI}$	0.76	0.82	$a + b \times \text{BI} + c \times \text{MSAVI}^2$	0.66	0.91

is due to variation observed in the relationship between LST and the SI for the present land cover in areas of study. The ratio of RMSE to the standard deviation (SD) shown in Table 6 for the four study areas shows value quite lower than 1 which reveals high degree of accuracy in the downscaled MODIS image.

Figures 5, 6, 7 and 8 represent the original MODIS-LST, downscaled MODIS-LST and the error in LST for Bikaner, Hyderabad, Vadodara and Varanasi, respectively. The error in LST was obtained from the difference of downscaled MODIS-LST and the reference-Landsat-LST. The downscaled MODIS-LST image was obtained from the best among the regression models for the four cities. The higher LST pixels in Bikaner showed positive error > 1, whereas the urban region having mixing pixels of vegetation and bare soil showed negative error < − 1. The water and its nearby pixels in Hyderabad show negative error < − 1. The bare region surrounding the city showed positive error. Similarly, the lowest LST pixels of water and vegetation in Vadodara showed negative error, whereas some pixels of bare land showed positive error. The water body showed positive error > 1, whereas the sandy area at the bank of river Ganga showed negative error < −1. Hence, it was observed that the greater error in LST was observed in pixels with extreme (highest for bare land/sand and lowest for water bodies) LST values, whereas the other land covers showed very low or negligible error in LST. The neighbouring land cover to these extreme LST pixels also showed larger error due to mixing of land covers with higher LST difference in a MODIS pixel.

5 Discussion

5.1 Behaviour of single SI used for downscaling in different cities

The downscaling results of MODIS-LST obtained using single SI were compared with the reference-Landsat-LST to assess the performance of each SI in different cities. The SD of the reference-Landsat-LST image was found to be 2.97, 2.87, 2.85 and 2.47 of Bikaner, Vadodara, Hyderabad and Varanasi, respectively. Hence, the RMSE values were found significantly below the SD of the reference-LST image for the four study areas except for NDSI in the Varanasi. The urban land covers and bare land are highly sensitive to SWIR bands. The indices NDBI, NDSI, UI and BI contain SWIR band for their determination. Thus, built-up and soil indices may explain better land cover variation in Bikaner, Vadodara and Hyderabad as compared with other indices. This resulted in improved downscaling results for the built-up/soil indices. Varanasi constitutes of vegetation and urban region as the major land cover. Vegetation is highly sensitive to NIR band. SWIR and NIR band were involved in the calculation of NDBI, UI and BI, whereas not in case of NDSI. Hence, NDSI does not have much potential to explain land cover variation in Varanasi resulting in a very high RMSE for downscaling of MODIS-LST. Therefore, NDBI, UI and BI have the capability to consider the land cover variations in the four different cities under study providing improvement in the downscaling results (Ogashawara and Bestos 2012).

Table 6 The ratio of the best RMSE to the SD determined from the downscaled MODIS-LST image and the reference-Landsat-LST image. The SD for each reference-Landsat-LST was also reported

	Bikaner	Hyderabad	Vadodara	Varanasi
Reference-Landsat-LST SD (K)	2.97	2.87	2.85	2.47
RMSE/SD	0.43	0.36	0.26	0.25

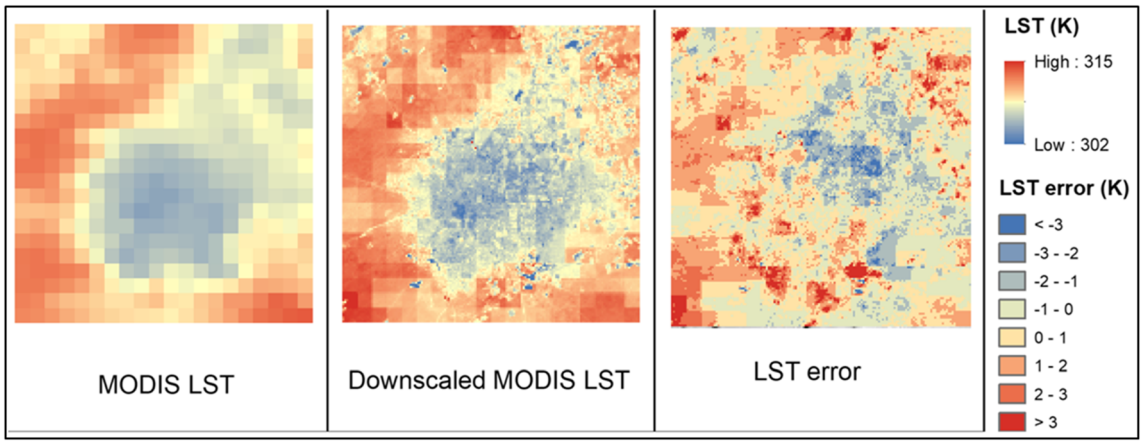

Fig. 5 The original MODIS-LST, downscaled MODIS-LST obtained using the transfer function $a + b \times \mathrm{NDVI}^2 + c \times \mathrm{BI}$ and the error in LST map of Bikaner

However, the performance of downscaled MODIS-LST was found to vary for different cities due to its dependence on relation of LST with different SI on the type of land cover available in a region. Previous work concluded that NDBI performed better than other SI for all the seasons in mixed urban landscapes (Govil et al. 2019), whereas NDSI was found suitable for downscaling LST in arid regions (Pan et al. 2018). The LST-NDVI relation was found useful for agricultural or vegetated areas (Eswar et al. 2016; Mukherjee et al. 2014), whereas built-up or soil indices were found useful for urban areas (Chen et al. 2013; Bala et al. 2018). Therefore, the results obtained from the present analysis were found in agreement with the previous work on downscaling of MODIS-LST.

5.2 Behaviour of LST for different land covers

The behaviour of LST varies for different land covers depending upon the heat capacity of the material (Rasul et al. 2017). The amount of energy or heat required to increase or decrease the temperature of a system by 1 K is known as heat capacity. Water bodies show the lowest LST values due to its high heat capacity (4.2 kJ kg^{-1} K^{-1}) and bare soil/sand or granite rocks show highest LST values due to their low heat capacity (0.8 kJ kg^{-1} K^{-1}). The heat capacity values of urban built-up materials lie in the range of (0.9–1.7 kJ kg^{-1} K^{-1}). The vegetated land cover showed lower LST values due to its tendency of evapotranspiration (Rinner and Hussain 2011).

The greater heat capacity of urban materials as compared with the desert area resulted to formation of UHS in Bikaner. Hyderabad City shows various low LST pixels due to the presence of numerous lakes within the city. The presence of hills made up of granite rocks with lower heat capacity shows higher LST values as compared with that of built-ups and is non-uniformly distributed within and outside the city. The high LST pixels within the city due to the presence of hills prevented the formation of UHS in Hyderabad City. The presence of bare land as well as sparse vegetated land in Vadodara resulted to lower

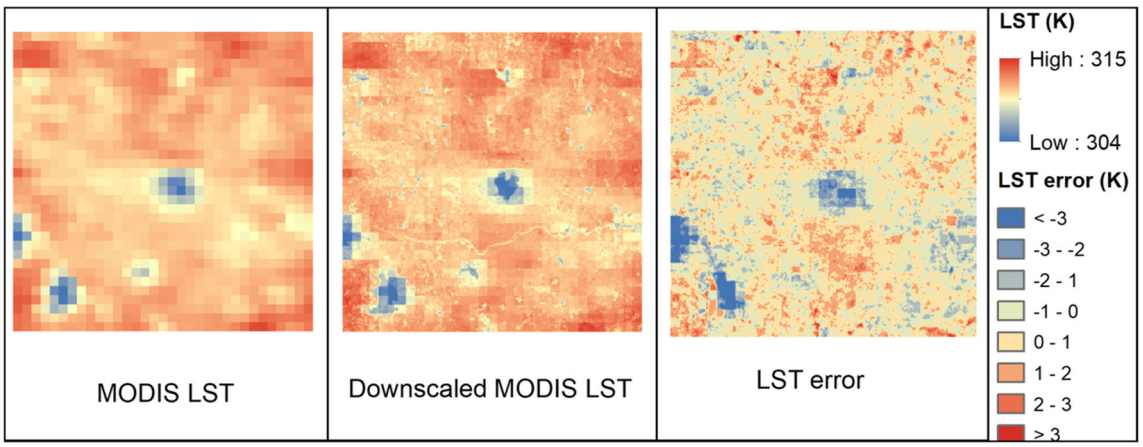

Fig. 6 The original MODIS-LST, downscaled MODIS-LST obtained using the transfer function $a + b \times \mathrm{NDVI}^2 + c \times \mathrm{BI}$ and the error in LST map of Hyderabad

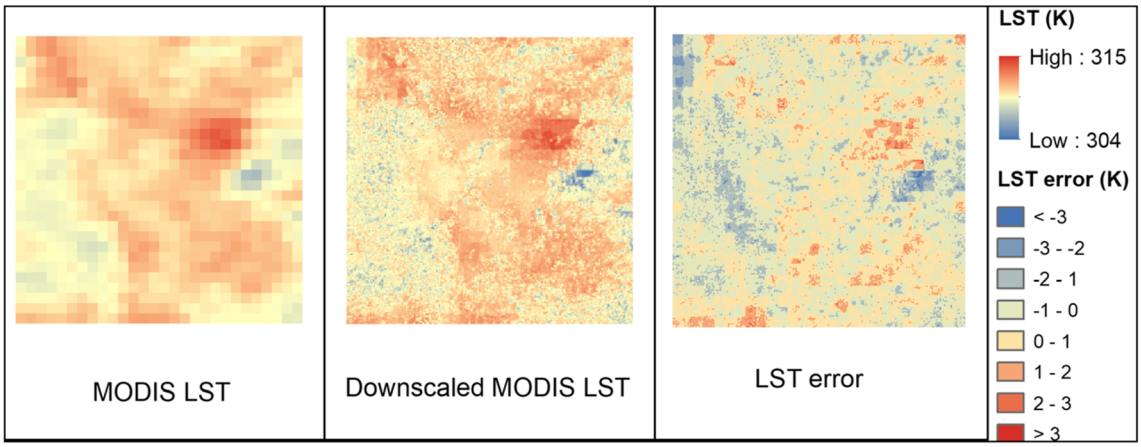

Fig. 7 The original MODIS-LST, downscaled MODIS-LST obtained using the transfer function $a + b \times \text{NDVI}^2 + c \times \text{NDSI}$ and the error in LST map of Vadodara

variation in the urban and rural land cover. The higher LST of urban land cover than the vegetation or water bodies resulted to UHI formation in Varanasi.

5.3 Comparative analysis of downscaling MODIS-LST in different cities

The downscaled MODIS-LST from single SI showed best result when using NDBI with RMSE value of 1.5 K and the result obtained from multiple linear regression showed best result with RMSE of 1.27 K in Bikaner. The downscaling of MODIS-LST showed best result when using BI with RMSE value of 0.92, 1.13 and 0.95, whereas multiple linear regression showed best result with RMSE of 0.73, 1.02 and 0.62 in Vadodara, Hyderabad and Varanasi, respectively. Thus, the multiple regression based thermal sharpening method was found to show improvement in the downscaling of MODIS-LST in the four cities. The combination of vegetation and built-up or soil indices was found useful for the disaggregation of MODIS-LST in heterogeneous urban landscapes. The fundamental contribution was provided by built-up/soil indices as indicated by the computed RMSE and was also confirmed by the greater value of the multiplicative coefficient of built-up/soil indices. The built-up indices include contribution from the bare land and urban land cover and vegetation indices include contribution from the vegetated land cover. The combination of both the indices results in improvement in the downscaling result.

The greater heterogeneity in land cover was observed in Hyderabad than other cities due to the presence of water body, bare land and vegetation in the urban areas. Vadodara has mixing of bare soil and vegetation in the urban areas. So, Vadodara has lower heterogeneity in land cover than Hyderabad. Bikaner and Varanasi have comparatively lower heterogeneity in the land cover surroundings than other study locations. This resulted in higher correlation coefficient (R) in Varanasi and Bikaner in comparison with Hyderabad and Vadodara. RMSE values were found lower in Varanasi and Vadodara in comparison with Hyderabad and Bikaner. The mixing of land covers with greater difference in LST in one MODIS pixel resulted to greater error in the downscaled MODIS-LST image.

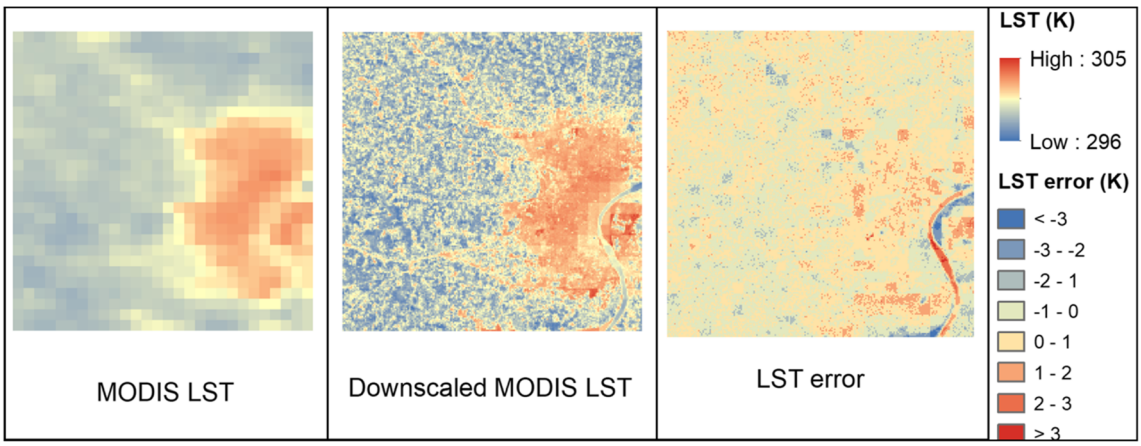

Fig. 8 The original MODIS-LST, downscaled MODIS-LST obtained using the transfer function $a + b \times \text{NDVI}^2 + c \times \text{NDBI} + d \times \text{EVI}^2$ and the error in LST map of Varanasi

Bikaner and Hyderabad consist of greater number of pixels with extreme LST values as compared with Vadodara and Varanasi cities. The mixing of low and high LST land covers within a MODIS pixel was observed in all the four cities. Thus, larger number of pixels was observed to show greater error in LST in Bikaner and Hyderabad as compared with other study areas. This result was also found consistent with RMSE value obtained by comparing the downscaled MODIS-LST image and the reference-Landsat-LST image for the four cities. Therefore, cities having greater number of pixels with extreme LST values and mixing of land covers within a MODIS pixel with higher difference in LST showed error in the downscaling of LST. However, the ratio of RMSE to SD reveals higher degree of accuracy for the downscaling results in the four study areas.

The combination of vegetation and built-up/soil indices includes the major contribution from all the land covers which resulted to better downscaling of MODIS-LST in the cities having distinct natural surroundings. Therefore, this statistical method for downscaling of MODIS-LST may be reasonably worthwhile for accurate mapping of LST image at FR on daily basis for various environmental applications.

6 Conclusions

The major concern of this paper is to study on the thermal sharpening of CR LST image from MODIS (~ 930 m) to a FR of 100 m for various heterogeneous urban landscapes. The cities with different climatic zones in India selected for this study are Bikaner, Vadodara, Hyderabad and Varanasi. The LST images generated from MODIS data were downscaled by establishing LST relation with the individual SI. Among the SI used in this study, NDBI, UI and BI showed better disaggregation results in comparison with the other indices for four study areas. Further, the statistical downscaling approach was carried out using the relation of LST with combination of the indices for disaggregation of MODIS-LST images. The combination $a + b \times \mathrm{NDVI}^2 + c \times \mathrm{BI}$ was observed best among the regression models to downscale MODIS-LST in Bikaner and Hyderabad cities. The combination $a + b \times \mathrm{NDVI}^2 + c \times \mathrm{NDSI}$ was found best to downscale LST in Vadodara, whereas the combination $a + b \times \mathrm{NDVI}^2 + c \times \mathrm{NDBI} + d \times \mathrm{EVI}^2$ showed best regression model to downscale MODIS-LST in Varanasi City. Hence, the best combination of indices for disaggregating LST images was found to vary for different cities indicating its dependence on the existence of the kind of land cover in a region. The regression model used for downscaling of MODIS-LST includes both vegetation and built-up/soil indices. The fundamental contribution is provided by the built-up/soil index which can be confirmed from the larger value of the multiplicative coefficient of built-up/soil indices as compared with that of vegetation indices.

The performance of the downscaled MODIS-LST was evaluated by comparing it with the reference-Landsat-LST to determine the R and the RMSE values. The R values obtained were 0.84, 0.76, 0.83 and 0.92 and the corresponding RMSE values were 1.27, 1.02, 0.73 and 0.62 for Bikaner, Vadodara, Hyderabad and Varanasi, respectively. The decrease in R value was observed with increase in heterogeneity of land cover in an urban area. This explains the lower value of R for Hyderabad having higher heterogeneity than other cities. The increase in RMSE value was observed due to the mixing of land covers with large difference in LST in a MODIS pixel. This resulted to higher RMSE values in Bikaner and Hyderabad in comparison with Vadodara and Varanasi. The RMSE for downscaled LST was found to show values quite lower than the SD of each reference-LST image revealing good degree of accuracy of downscaled LST image.

The selective use of combination of both vegetation and built-up or soil indices proves to be convenient for thermal sharpening in different urban areas. Therefore, this method can be effectively used for thermal sharpening of LST with CR for mapping of LST at FR accurately in different heterogeneous urban areas for various applications. However, the study has been performed on four different cities and the best combinations of SI were found to vary for different cities. Further studies must be performed over different heterogeneous urban regions to obtain a broad overview of the use of SI in thermal sharpening techniques with increased accuracy.

Acknowledgements The authors would like to thank the Department of Physics, Indian Institute of Technology (BHU), Varanasi, India for providing a research platform and also Council of Scientific and Industrial Research (CSIR), New Delhi, India for providing the financial support.

References

Agam N, Kustas WP, Anderson MC, Li F, Colaizzi PD (2007a) Utility of thermal-sharpening over Texas high plains irrigated fields. J Geophys Res 112:D19110. https://doi.org/10.1029/2007JD008407

Agam N, Kustas WP, Anderson MC, Li F, Neale MU (2007b) A vegetation index based technique for spatial sharpening of thermal imagery. Remote Sens Environ 107:545–558. https://doi.org/10.1016/j.rse.2006.10.006

Atkinson PM (2013) Downscaling in remote sensing. Int J Appl Earth Obs Geoinf 22:106–114. https://doi.org/10.1016/j.jag.2012.04.012

Bala R, Prasad R, Yadav VP, Sharma J (2018) A comparative study of land surface temperature with different indices on heterogeneous land-cover using Landsat 8 Data. Int Arch Photogramm Remote Sens Spat Inf Sci XLII-5:389–394. https://doi.org/10.5194/isprs-archives-XLII-5-389-2018

Bala R, Prasad R, Yadav VP (2019) Disaggregation of modis land surface temperature in urban areas using improved thermal-sharpening techniques. Adv Space Res 64:591–602. https://doi.org/10.1016/j.asr.2019.05.004

Barsi JA, Schott JR, Palluconi FD, Hook SJ (2005) Validation of a web-based atmospheric correction tool for single thermal band instruments. Proc. SPIE, Bellingham, WA, USA, vol. 5882, Paper 58820E, pp. 1–7. https://doi.org/10.1117/12.619990

Bonafoni S (2016) Downscaling of Landsat and MODIS land surface temperature over the heterogeneous urban area of Milan. IEEE J Sel Topics Appl Earth Observ Remote Sens 9(5):2019–2027. https://doi.org/10.1109/JSTARS.2016.2514367

Chen L, Li M, Huang F & Xu S (2013) Relationships of LST to NDBI and NDVI in Wuhan City based on Landsat ETM+ image. In 2013 6th International Congress on Image and Signal Processing (CISP) (Vol. 2, pp. 840-845). IEEE. https://doi.org/10.1109/CISP.2013.6745282

Essa W, Verbeiren B, Van Der Kwast J, Van De Voorde T, Batelaan O (2012) Evaluation of the Distrad thermal-sharpening methodology for urban areas. Int J Appl Earth Obs Geoinf 19:163–172. https://doi.org/10.1016/j.jag.2012.05.010

Eswar R, Sekhar M, Bhattacharya BK (2016) Disaggregation of LST over India: comparative analysis of different vegetation indices. Int J Remote Sens 37(5):1035–1054. https://doi.org/10.1080/01431161.2016.1145363

Govil H, Guha S, Dey A, Gill N (2019) Seasonal evaluation of downscaled land surface temperature: a case study in a humid tropical city. Heliyon 5(6):e01923. https://doi.org/10.1016/j.heliyon.2019.e01923

Jeganathan C, Hamm NAS, Mukherjee S, Atkinson PM, Raju PLN, Dadhwal VK (2011) Evaluating a thermal image sharpening model over a mixed agricultural landscape in India. Int J Appl Earth Obs Geoinf 13:178–191. https://doi.org/10.1016/j.jag.2010.11.001

Julien Y, Sobrino JA (2009) The Yearly Land-cover Dynamics (YLCD) method: an analysis of global vegetation from NDVI and LST parameters. Remote Sens Environ 113:329–334. https://doi.org/10.1016/j.rse.2008.09.016

Justice CO, Giglio L, Korontzi S, Owens J, Morisette JT, Roy D, Descloitres J, Alleaume S, Petitcolin F, Kaufman Y (2002). The MODIS fire products. Remote SensEnviron 83: 244–262. https://doi.org/10.1016/S0034-4257(02)00076-7

Kauffman RK, Seto KC, Schneider A, Liu Z, Zhou L, Wang W (2007) Climate response to rapid urban growth: evidence of a human-induced precipitation deficit. J Clim 20:2299–2306. https://doi.org/10.1175/JCLI4109.1

Kustas WP, Norman JM, Anderson MC, French AN (2003) Estimating subpixel surface temperatures and energy fluxes from the vegetation index-radiometric temperature relationship. Remote Sens Environ 85:429–440. https://doi.org/10.1016/S0034-4257(03)00036-1

Liu K, Fang J, Zhao D, Liu X, Zhang X, Wang X, Li X (2016) An assessment of urban surface energy fluxes using a sub-pixel remote sensing analysis: a case study in Suzhou, China. ISPRS Int J Geo-Inf 5:11. https://doi.org/10.3390/ijgi5020011

Mukherjee S, Joshi PK, Garg RD (2014) A comparison of different regression models for downscaling Landsat and MODIS land surface temperature images over heterogeneous landscape. Adv Space Res 145:55–67. https://doi.org/10.1016/j.asr.2014.04.013

Mukherjee S, Joshi PK, Garg RD (2017) Analysis of urban built-up areas and surface urban heat island using downscaled MODIS derived land surface temperature data. Geocarto Int 32(8):900–918. https://doi.org/10.1080/10106049.2016.1222634

Nuruzzaman M (2015) Urban heat island: causes, effects and mitigation measures-a review. Int J Environ Monit Anal 3(2):67–73. https://doi.org/10.11648/j.ijema.20150302.15

Pan X, Zhu X, Yang Y, Cao C, Zhang X, Shan L (2018) Applicability of downscaling land surface temperature by using normalized difference sand index. Sci Rep 8(1):9530. https://doi.org/10.1038/S41598-018-27905-0

Rajasekar U, Weng Q (2009) Urban heat island monitoring and analysis using a non parametric model: a case study of Indianapolis ISPRS J. Photogramm Remote Sens 64:86–96. https://doi.org/10.1016/j.isprsjprs.2008.05.002

Rasul A, Balzter H, Smith C, Remedios J, Adamu B, Sobrino JA, Srivanit M, Weng Q (2017) A review on remote sensing of urban heat and cool islands. Land. 6:38. https://doi.org/10.3390/land6020038

Rinner C, Hussain M (2011) Toronto's urban heat island—exploring the relationship between land use and surface temperature. Remote Sens 3(6):1251–1265. https://doi.org/10.3390/rs3061251

Stathopoulou M, Cartalis C (2009) Downscaling AVHRR land surface temperatures for improved surface urban heat island intensity estimation. Remote Sens Environ 113(15):2592–2605. https://doi.org/10.1016/j.rse.2009.07.017

Steven MD, Malthus TJ, Baret F, Xu H, Chopping MJ (2003) Intercalibration of vegetation indices from different sensor systems. Remote Sens Environ 88(4):412–422. https://doi.org/10.1016/j.rse.2003.08.010

Van de Griend AA, Owe M (1993) On the relationship between thermal emissivity and the normalized difference vegetation index for natural surfaces. Int J Remote Sens 14:1119–1131. https://doi.org/10.1080/01431169308904400

Voogt JA, Oke TR (2003) Thermal remote sensing of urban climates. Remote Sens Environ 86:370–384. https://doi.org/10.1016/S0034-4257(03)00079-8

Wang L, Qu JJ (2009) Satellite remote sensing applications for surface soil moisture monitoring: a review. Front Earth Sci China 3(2):237–247. https://doi.org/10.1007/s11707-009-0023-7

Weng Q (2009) Thermal infrared remote sensing for urban climate and environmental studies: methods, applications and trends. ISPRS J Photogramm Remote Sens 64:335–344. https://doi.org/10.1016/j.isprsjprs.2009.03.007

Yang Y, Li X, Pan X, Zhang Y, Cao C (2017) Downscaling land surface temperature in complex regions by using multiple scale factors with adaptive thresholds. Sensors 17:744. https://doi.org/10.3390/s17040744

Yao R, Wang L, Huang X, Niu Z, Liu F, Wang Q (2017) Temporal trends of surface urban heat islands and associated determinants in major Chinese cities. Sci Total Environ 609:742–754. https://doi.org/10.1016/j.scitotenv.2017.07.217

Yao R, Wang L, Huang X, Chen J, Li J, Niu Z (2018) Less sensitive of urban surface to climate variability than rural in Northern China. Sci Total Environ 628-629:650–660. https://doi.org/10.1016/j.scitotenv.2018.02.087

Zhan W, Chen Y, Zhou J, Wang J, Liu W, Voogt J, Zhu X, Quan J, Li J (2013) Disaggregation of remotely sensed land surface temperature: literature survey, taxonomy, issues, and caveats. Remote Sens Environ 131:119–139. https://doi.org/10.1016/j.rse.2012.12.014

Zhang Y, Odeh IOA, Han C (2009) Bi-temporal characterization of land surface temperature in relation to impervious surface area, NDVI and NDBI, using a sub-pixel image analysis. Int J Appl Earth Obs Geoinf 11:256–264. https://doi.org/10.1016/j.jag.2009.03.001

Zhang D, Tang R, Tang B, Wu B, Li Z (2015) A simple method for soil moisture determination from LST–VI feature space using nonlinear interpolation based on thermal infrared remotely sensed data. IEEE J Sel Topics Appl Earth Observ Remote Sens 8:2. https://doi.org/10.1109/JSTARS.2014.2371135

Zhou D, Xiao J, Bonafoni S, Berger C, Deilami K, Zhou Y, Frolking S, Yao R, Qiao Z, Sobrino J (2019) Satellite remote sensing of surface urban heat islands: progress, challenges, and perspectives. Remote Sens 11:48. https://doi.org/10.3390/rs11010048